Refractometric sensor based on a phase-shifted long-period fiber grating

Rosane Falate, Orlando Frazão, Gaspar Rego, José Luís Fabris, and José Luís Santos

A refractometric sensor based on a phase-shifted long-period fiber grating written by electric-arc discharges is presented. Transmission and reflective configurations for refractive index measurements are studied. It is observed that the reflective topology permits better performance compared with the transmission one, which is the approach normally utilized in the context of long-period fiber sensing. The resolution achieved in the measurement of refractive index enables the application of this sensing head structure in demanding situations, such as the measurement of the level of salinity of water.

OCIS codes: 050.2770, 050.5080, 060.2370, 060.2340.

1. Introduction

Long-period fiber gratings (LPFGs) are devices that share the intrinsic characteristics of optical fiber sensors, such as electrically passive operation, immunity to electromagnetic radiation, and multiplexing capability, and some specific characteristics such as low backreflection and low insertion loss. The low backreflection characteristic occurs because LPFGs operate in transmission owing to the coupling of the fundamental guided mode to codirectional cladding modes.[1] The coupling between forward modes occurs when the phase-matching vector ($\Delta\beta$) is short, which corresponds with a spatial modulation period of a hundred micrometers for LPFG fabrication, a practical advantage compared with fiber Bragg gratings.

The large spatial period of LPFGs has enabled the development of different fabrication techniques. In fact, for instance, LPFGs can be obtained using ultraviolet (UV) irradiation,[1,2] infrared CO_2 laser radiation,[3] electric-arc discharges,[4] and mechanical pressure.[5] The writing processes that use the point-to-point technique can produce a complex pattern in the refractive index modulation along the fiber since, after each point, the writing parameters can be changed. This property can easily be used to explore new LPFG structures, such as phase-shifted LPFGs,[6] Mach–Zehnder interferometry using LPFGs,[6] or superstructured fiber Bragg gratings.[7]

An interesting characteristic of LPFGs is their sensitivity to the refractive index of the environment where they are immersed. Several authors have proposed different configurations of refractometric sensors based on LPFGs. The simplest configuration, which consists of an optical broadband source, a single LPFG immersed in the liquid under analysis, and an optical spectrum analyzer, has been studied by several authors. Lee *et al.*[8] demonstrated a new method of analysis to determine the spectral displacement of the LPFG as a function of the ambient refractive index. Patrick *et al.*[9] presented the wavelength variation of the LPFG attenuation band with changes of this parameter. Measurements of external refractive indices using higher-order cladding modes have been performed by Shu *et al.*[10] Gwandu *et al.*[11] proposed a compact scheme for simultaneous temperature and surrounding refractive index measurement using two LPFGs inscribed in a hydrogenated double-cladding fiber, while Duhem *et al.*[12] also used two LPFGs, but to

R. Falate (rfalate@yahoo.com) is with Universidade Tecnológica Federal do Paraná, Avenida Sete de Setembro 3165, 80230-901 Curitiba, Brazil, and Unidade de Optoelectrónica e Sistemas Electrónicos, INESC-Porto, Rua do Campo Alegre 687, 4169-007 Porto, Portugal. O. Frazão is with Unidade de Optoelectrónica e Sistemas Electrónicos, INESC-Porto, Rua do Campo Alegre 687, 4169-007 Porto, Portugal. G. Rego is with Escola Superior de Tecnologia e Gestão, Instituto Politécnico de Viana do Castelo, Avenida do Atlântico, 4900-348 Viana do Castelo, Portugal, and Unidade de Optoelectrónica e Sistemas Electrónicos, INESC-Porto, Rua do Campo Alegre 687, 4169-007 Porto, Portugal. J. L. Fabris is with Universidade Tecnológica Federal do Paraná, Avenida Sete de Setembro 3165, 80230-901 Curitiba, Brazil. J. L. Santos is with Unidade de Optoelectrónica e Sistemas Electrónicos, INESC-Porto, Rua do Campo Alegre 687, 4169-007 Porto, Portugal, and Departamento de Física, Faculdade de Ciências da Universidade do Porto, Rua do Campo Alegre, 687, 4169-007 Porto, Portugal.

Received 20 December 2005; revised 29 March 2006; accepted 30 March 2006; posted 4 April 2006 (Doc. ID 66613).

0003-6935/06/215066-07$15.00/0

produce a Mach–Zehnder interferometer with its path imbalance modulated by the environmental refractive index. Swart *et al.*[13] attained the same objective using a LPFG in a self-interference Michelson configuration to obtain a channeled spectrum with narrow bandwidth fringes. This concept, which relies on the implementation of a reflective surface at the end of the optical fiber nearby the LPFG (a silver layer or, simply, the Fresnel reflection when the maximization of the optical power level is not of concern), is very interesting because it transforms the long-period based fiber sensing head with two fiber ends into a fiber probe with reduced size, facilitating the packaging process and simplifying its use in different measurement situations.

In this work a refractometric sensing head based on a phase-shifted long-period fiber grating is presented. Transmission and reflective configurations are studied and compared. A specific but important application is afterward demonstrated, namely, the ability of this sensing head structure to measure the salinity level of water.

2. Experimental Results

A. Phase-Shifted Long-Period Fiber Grating Fabrication

The transmission spectral characteristics of long-period fiber grating structures can be changed when two LPFG sections, with same grating period (Λ), are placed together with a length separation L_p between them. If this optical fiber length does not have the fiber buffer layer (acrylate coating), the resultant device will be a Mach–Zehnder interferometer when $L_p > \Lambda$; otherwise, if $L_p < \Lambda$, a phase-shifted long period fiber grating (PS-LPFG) will result. The analysis of phase-shifted long-period fiber gratings developed by Ke *et al.*[14] was experimentally explored by Humbert and Malki for LPFG written processes that use the point-to-point technique.[15] Besides the detailed description of the experimental procedures for the production of high-performance phase-shifted long-period gratings by electric-arc discharges, they also gave the formula for the phase-shift value: $\Delta\phi = 2\pi L_p/\Lambda$, where $\Delta\phi$ is the desired phase-shift value in radians.

The experimental setup used to fabricate the phase-shifted long-period gratings is the same described by Rego *et al.*[4] An uncoated Corning SMF-28 fiber is placed between the electrodes of a fusion splice machine. To keep the fiber under constant axial stress, a small weight is suspended in one of the fiber ends, while the other is clamped in a fiber holder on top of a motorized translation stage computer controlled with a precision of 0.1 μm. An electric arc is then applied with an electric current of 8.5–10.0 mA during 0.5–2.0 s, exposing a short length of the fiber. After the discharge, the translation stage displaces the fiber by a distance that represents the grating period (Λ), typically 400–700 μm, several times (N) until a required attenuation loss peak is obtained. The gratings spectra were recorded using an optical spectra analyzer (OSA) set to a resolution of 1.0 nm. The illumination was provided by a white light source.

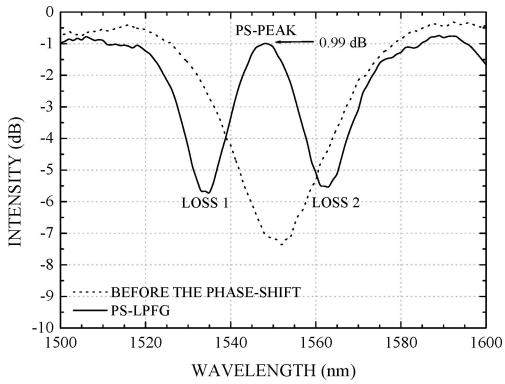

Fig. 1. Transmission spectrum of the LPFG structure before the phase shift to be applied (dotted curve) and at the final of the writing process (solid curve).

For the particular PS-LPFGs produced for the present work, the following set of fabrication parameters were used: weight of 5.1 g; period of 540 μm; electric current of 9.5 mA; arc duration of 1 s. The first LPFG section was fabricated up to the point where the transmission loss at the resonance wavelength was approximately 6.9 dB, corresponding to approximately 35 electric discharges. When this point was reached, the fiber was translated by $L_p = 118$ μm to introduce the required phase shift and, afterwards, the writing process was repeated for the second LPFG section until the desired transmission spectrum was reached. The total number of electric discharges was 70, and the total grating structure had a length of $(N - 1)\Lambda + L_p$. Figure 1 shows the transmission spectrum before the insertion of the phase shift and at the end of the fabrication process. The final transmission spectrum shows two band rejection peaks: the first one is at 1534 nm (referred to as LOSS 1), and the second one is at 1562 nm (LOSS 2). The bandpass peak (PS-PEAK), between the two band-rejection peaks, is at 1548 nm. The bandwidth FWHM (full width half-maximum) of the fabricated PS-LPFG is 18.5 nm, and the insertion loss is 0.99 dB.

B. Transmission Configuration

Figure 2(a) shows the experimental setup used to test the sensing head based on a phase-shifted LPFG in a transmission configuration. The PS-LPFG sensor was inserted into an immobile plastic recipient with four openings, two of them used to insert the optical fiber with the PS-LPFG, and the two others to insert and to drain the liquid samples. Then, after the PS-LPFG had been inserted into the recipient, the fiber ends were held to avoid fiber-bending effects on the sensor response. Another parameter controlled to minimize measurement errors was the room temperature, which was kept at ~19 °C. Finally, to obtain the transmission spectra of the PS-LPFG sensor, a broadband optical source (BBOS), an erbium-doped fiber amplifier (EDFA model FIBREAMP-BT 1400

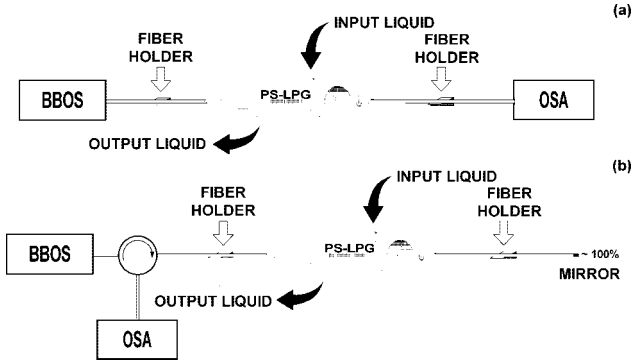

Fig. 2. Experimental setup used to test sensing heads based on a phase-shifted LPFG in (a) transmission and (b) reflective configurations (the parameter under measurement is the refractive index of a liquid).

from Photonetics with a gain bandwidth of 100 nm around 1550 nm), and an optical spectra analyzer (OSA, model AQ-6315B from Ando) were used. The refractive index range for the studied samples was between 1.32 and 1.44. These refractive index values were measured with an Abbe refractometer working at 589 nm just after the samples had been drained of the plastic recipient. The Cauchy equation can be used to obtain the refractive index of these samples at the PS-LPFG operation wavelength (1550 nm).[16]

Figure 3 shows the wavelength shifts for the three resonances labeled LOSS 1, LOSS 2, and PS-PEAK in Fig. 1, as a function of the refractive index of the surrounding liquid. These results are in line with previous ones presented by other authors. The resonance peaks shift to lower wavelengths when the external refractive index increases, with the resonance LOSS 2 exhibiting a marginally higher sensitivity when compared with the other two due to its spectral location at longer wavelengths.

C. Reflective Configuration

The experimental setup implemented to test the reflective configuration is shown in Fig. 2(b). Compared with the transmission layout [Fig. 2(a)], an optical circulator was included to read the optical spectra in reflection and, at the end of the optical fiber, a silver coating was deposited with a reflectivity of ≈100%.

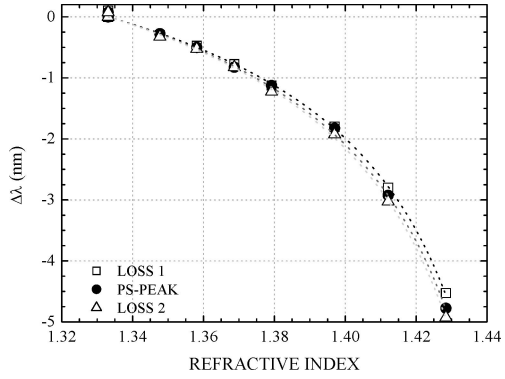

Fig. 3. Refractive index wavelength response of the PS-LPFG based sensing head operating in the transmission configuration.

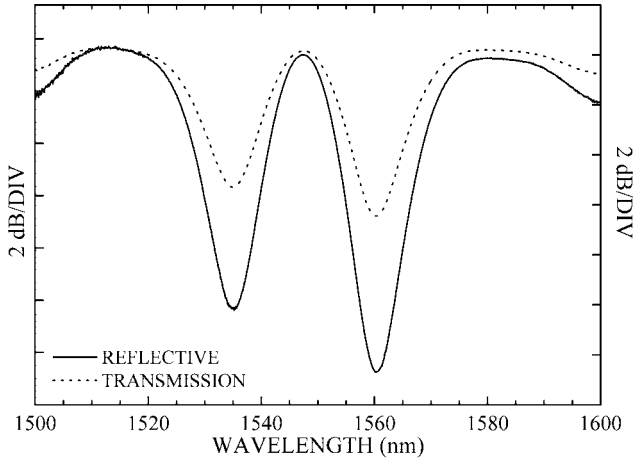

Fig. 4. Comparison between the transmission spectrum (dotted curve) and the reflective spectrum (solid curve) of the phase-shifted LPFG structure.

When the light propagates the first time through the PS-LPFG, the wavelengths in the grating LOSS 1 and LOSS 2 resonance bands are coupled into cladding modes to a variable degree, while the other wavelengths continue to travel in the fiber core toward the mirror located at the end of the cleaved fiber. The light that propagates in the cladding modes is leaked out, a process assisted by the fiber coating between the PS-LPFG and the mirror, which is not removed. On reflection in the mirror, the core wave retraces its path toward the PS-LPFG. At the grating, part of the core wave is coupled again to cladding modes that are, by the second time, lost due to the cladding–external medium interface. Therefore, in the spectral regions where the mode coupling occurs, the core light is leaked out twice; out of these spectral regions the amplitude does not change since the light is always kept in the core. The net result of this process is a sharpness of the spectral PS-LPFG transfer function (Fig. 4), a feature that has positive consequences on the measurement performance of this configuration, as is shown below.

D. System Resolution

The optical power variation at the wavelength of 1552.8 nm as function of the refractive index of the external liquid for both the transmission and reflective configuration is shown in Fig. 5. It is interesting to note that the chosen wavelength value of 1552.8 nm, located in the right side region of the central resonance of the PS-LPFG, is not arbitrary. It was chosen after the analysis of the transmission spectral evolution of PS-LPFG for the desired refractive index operation range, between 1.3333 and 1.4283, and the search for a wavelength region where power changes are high but not maximum. This procedure is important to avoid detecting both sides of PS-LPFG resonance and, consequently, to obtain the same power value for two different refractive indexes, one due to the positive and another due to the negative slope.

As can be observed, the optical power variation in-

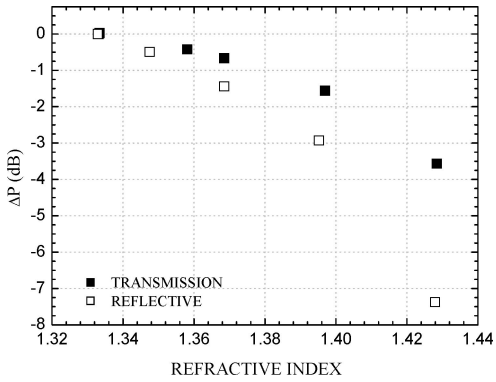

Fig. 5. Variation of the returned optical power at the wavelength 1552.8 nm, as a function of the refractive index of the external liquid, for the transmission and reflective topologies.

duced by changes of the refractive index approximately doubles for the reflective configuration. This is an expectable result in face of the light double propagation through the PS-LPFG. Considering that the insertion loss of the PS-LPFG structure operating in reflection does not increase substantially comparatived to the transmission configuration (Fig. 4), such double optical power variation translates almost directly into a double measurand resolution. On the other hand, the wavelength variations induced in the spectral structure by the external refractive index variations are essentially the same for the transmission and reflective configurations. This similarity comes from the fact that such wavelength shifts occur due to the change on the effective refractive index of the cladding, which is independent of the configuration used.

When the reading is in wavelength, even if the sensitivity of the sensing head for refractive index measurement is similar for the reflective and transmission configurations, the resolution is better in the former case. This result can be observed in Fig. 6, which shows the wavelength readout evolution for a fixed value of the refractive index of the surrounding medium (fixed sample), together with the step variations of the measured values when the sample under measurement is changed. This happens because the system refractive index readout resolution is determined not only by its intrinsic sensitivity to this parameter, but also by the noise level present, considering this factor affects the accuracy with which a particular spectral instrument (an OSA in this case) determines the wavelength of the resonance peaks of the PS-LPFG structure. For a fixed noise level, the fluctuations in the measured values of the resonance wavelength are smaller for the reflective configuration, compared with the transmission one, due to its sharper transfer function, i.e., the resonance peaks are better defined in presence of noise. Indeed, those fluctuations have rms values of 0.066 nm and 0.035 nm for the transmission and reflective topologies, respectively, indicating that the reflective layout provides a refractive index measurement resolution approximately a factor of 2 better than the transmission one.

The nonlinearly of PS-LPFG refractive index sensi-

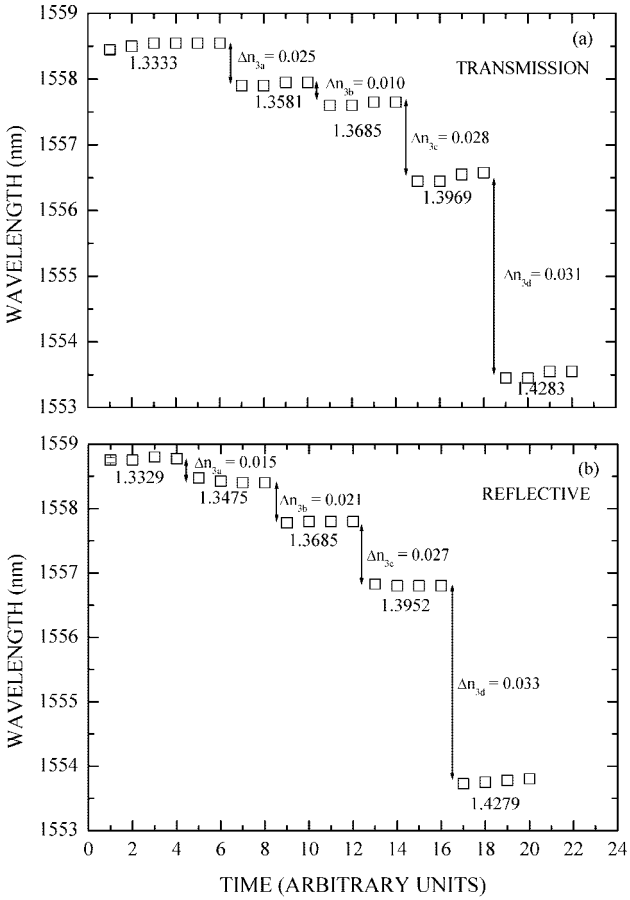

Fig. 6. Wavelength stability obtained during the refractive index measurements when the transmission and reflective configurations are used.

tivity (Fig. 3) forbids a linear translation from wavelength rms values into refractive index resolutions. Considering two refractive index regions around 1.37 and 1.40, the corresponding resolutions achieved were respectively 2.1×10^{-3} RIU (refractive index units) and 1.1×10^{-3} RIU for the transmission configuration, while for the reflective configuration such values became 1.1×10^{-3} RIU and 0.6×10^{-3} RIU, respectively. It is also interesting to note that for both the transmission and the reflective configurations, the grating was kept untouched even after the silver coating procedure, which was made in a fiber part distant from the plastic recipient.

E. Salinity Measurement

An important application of high-resolution refractive index sensors is the measurement of the degree of salinity of water. Usually, this parameter is determined using electrical conductivity techniques due to the presence of chlorine ions in the water solution.[17] However, the salinity can also be determined through measurement of the refractive index, since an empirical equation between the seawater salinity and its refractive index is well established.[17,18]

The refractive index range of water with a salinity level from zero to that present in seawater goes from

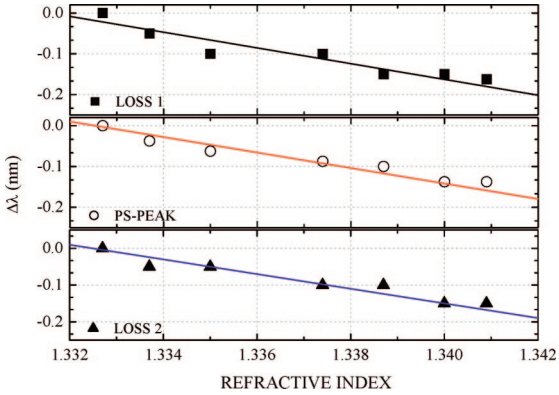

Fig. 7. (Color online) Wavelength sensitivities of the three PS-LPFG resonances, in the reflective configuration, when measuring refractive index in a range corresponding to a salinity level from zero to that present in seawater.

1.332 up to 1.342. This means that a relatively highly sensitive refractive index measurement technique is required to identify the water salinity level. Due to this need, the reflective PS-LPFG based configuration was used following the experimental setup shown in Fig. 2(b). Two measurement approaches were considered, namely, the measurand induced wavelength shifts and the measurand induced optical power variations at specific wavelengths.

Although wavelength and power are necessary parameters for refractive index determination of seawater using long-period grating devices, they are not sufficient when an absolute refractive index value is desired. This condition occurs because the long-period grating device not only measures the surrounding fiber refractive index but also other parameters that can change either the effective refractive index of core or the effective refractive index of cladding or both, such as temperature and strain. Furthermore, temperature also changes the refractive index of material under analysis, which generates an extra error in the measurement. Therefore, methods to avoid or to correct errors related to external physical parameters are necessary. For the reasons described before, during all experiments concerning the refractive index range of seawater, the room temperature was monitored and controlled to ensure changes up to 0.3 °C. This temperature variation corresponds to a wavelength error of ±11 pm considering a temperature sensitivity of 74 pm/°C.[19]

Figure 7 shows the wavelength responses for the three resonant bands of the PS-LPFG structure. It can be observed that for the refractive index range under concern, the wavelength shifts of these resonances are essentially linear and equal, with sensitivities of −19.30 ± 1.73 nm/RIU (resonance LOSS 1), −19.95 ± 1.50 nm/RIU (resonance LOSS 2), and −19.00 ± 1.41 nm/RIU (resonance PS-PEAK).

In the context of salinity measurement, the other approach that was explored was the measurand induced optical power variations at certain wavelengths. Compared with the case of wavelength-shift reading, this approach does not require specific equipment to detect wavelength variations, which is in general expensive, is conceptually simpler, and has the potential to provide similar or even better measurand resolutions. Its main drawback is its intrinsic susceptibility to errors arising from the presence of optical power variations others than those induced by the measurand. Due to this susceptibility to errors, it is necessary to couple to the scheme some type of optical power correction, following one of many solutions that have been proposed along the years to tackle this problem.

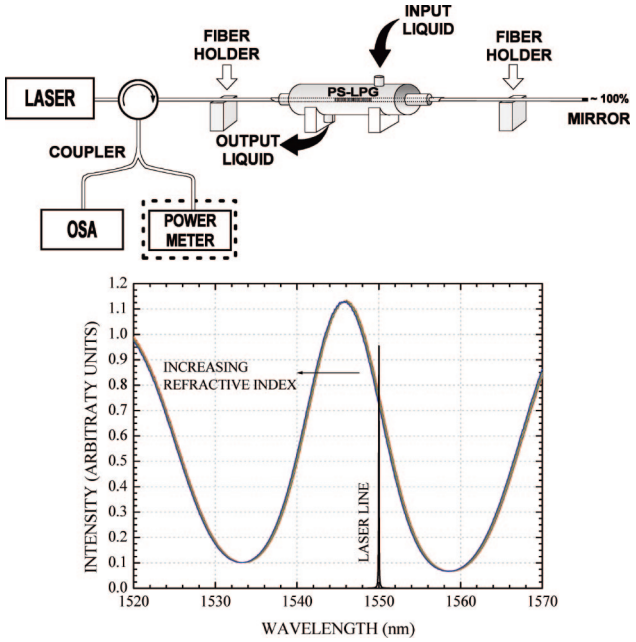

Fig. 8. (Color online) Experimental setup to measure the water salinity level through detection of measurand induced optical power variations (also shown is the relative position of the PS-LPFG spectral transfer function and of the laser line in one of the measurement situations).

Figure 8 shows the experimental setup implemented to test this approach in the context of salinity measurement. Compared with the setup of Fig. 2(b), two modifications were introduced: a tunable semiconductor laser (TSL-210 from Santec) was used as the optical source to have improved measurement flexibility (in a practical situation an inexpensive semiconductor laser diode would be enough), and the output port of the circulator was connected to an OSA and to an optical powermeter (OPM) through a coupler. Again, in a real situation both this coupler and the OSA would not be necessary, and a single photodetection and amplification block could work as an OPM. Figure 8 also shows the relative position of the PS-LPFG spectral transfer function and of the laser line in one of the measurement situations.

Figure 9 shows the results obtained with this configuration with the laser line at 1550 nm. The environment temperature was kept constant at the value 23.4 ± 0.1 °C. Due to the shift to shorter wavelengths

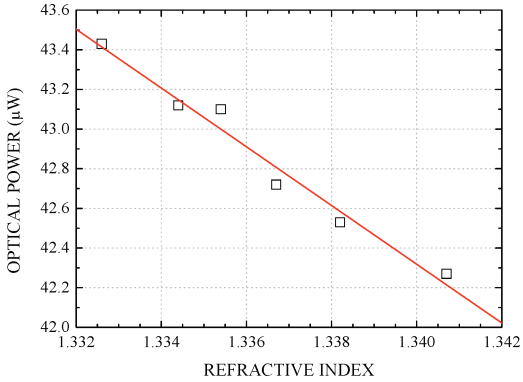

Fig. 9. (Color online) Variation of the detected optical power with the laser line at 1550 nm when the refractive index of water changes.

of the PS-LPFG spectrum when the refractive index of the liquid increases, there is a corresponding linear decrease of the detected optical power with a slope of -146.14 ± 7.20 μW/RIU. It is clear from these results that this measurement approach permits easy determination of the refractive index variations of water when its degree of salinity changes.

Actually, it is possible to improve the performance of this technique using the two sides of the central resonance of the PS-LPFG structure. In fact, when the refractive index changes, the optical powers in two wavelengths located on these sides vary in a symmetric way, i.e., one optical power increases while the other decreases. Therefore, if P_1 and P_2 represent these optical powers, then the processing $[(P_1 - P_2)/(P_1 + P_2)]$ essentially doubles the measurand readout sensitivity and, simultaneously, permits the correction of the optical power fluctuations along the system.

To test this approach, two laser sources were used, one emitting at $\lambda_1 = 1537.8$ nm (generating P_1) and the other at $\lambda_2 = 1552.8$ nm (generating P_2). These wavelengths are located at each side of the PS-LPFG spectral transfer function (see Fig. 8). The processing $[(P_1 - P_2)/(P_1 + P_2)]$ permits afterwards the results shown in Fig. 10. From this figure the excellent discrimination of the refractive index changes associated with the salinity range under concern is evident. On the other hand, there is also a degree of nonlinearity in the obtained results, a consequence of the implemented ratio. However, this feature is not of too much concern in face of two reasons. First, it is always possible to correct this nonlinearity with further signal processing. Second, and more relevant, the calibration function of Fig. 10 can be found to be linear by choosing proper values for λ_1 and λ_2. In principle, when practically feasible, this second alternative is the preferable one.

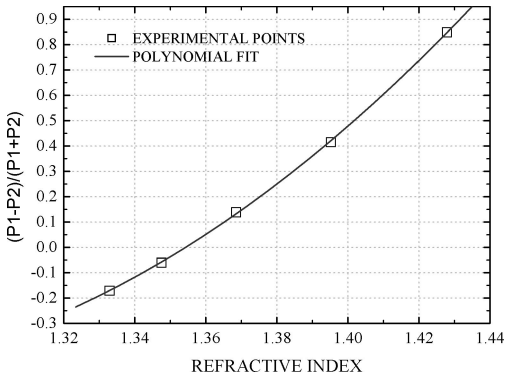

Fig. 10. Normalized optical power variation $[(P_1 - P_2)/(P_1 + P_2)]$ versus refractive index of water ($P_1 \rightarrow$ detected optical power at $\lambda_1 = 1537.8$ nm; $P_2 \rightarrow$ detected optical power at $\lambda_2 = 1552.8$ nm).

3. Conclusion

Arc-induced phase-shifted long-period fiber gratings in SMF-28 fiber were fabricated to measure external refractive indices. Transmission and reflective configurations were studied. The main advantage of using phase-shifted LPFG sensors instead of conventional LPGs is the positive peak presence in the transmission spectrum. Such a positive peak allows a high power level to be available when the wavelength measurement is performed with improvement in the signal-to-noise ratio of the refractive index measurement system. The measurand induced action was determined by monitoring both the wavelength shifts of the grating resonances and the optical power variations at specific wavelengths. It was observed that the reflective topology permits better performance compared with the transmission one, which is the approach normally utilized in the context of long-period fiber sensing. Also, the intensity based technique, which is conceptually simpler and technically less demanding, showed appreciable performance, particularly in the case where power correction was implemented. The phase-shifted long-period fiber grating structure in the reflective configuration was applied, with success, to measure the small refractive index variations associated with the degree of salinity of water up to the value found in seawater. This result, together with the intrinsic wavelength selectivity of the described grating device, makes viable the concretization of a fiber optic multiplexed sensing system for real-time monitoring of water salinity levels in delicate ecosystems, such as those found in sea-river lagoons.

R. Falate's work was supported in part by the Brazilian agencies Coordenação de Aperfeiçoamento de Pessoal de Nivel Superior, CAPES, and CNPq. G. Rego is thankful for a grant through the Program PRODEP III, Medida 5, Acção 5.3, Formação Avançada de Docentes do Ensino Superior.

References

1. V. Bhatia and A. M. Vengsarkar, "Optical fiber long-period grating sensors," Opt. Lett. **21,** 692–694 (1996).
2. S. W. James and R. P. Tatam, "Optical fiber long-period grating sensors: characteristics and application," Meas. Sci. Technol. **14,** R49–61 (2003).
3. D. D. Davis, T. K. Gaylord, E. N. Glytsis, S. G. Kosinski, S. C. Mettler, and A. M. Vengsarkar, "Long-period fibre grating fab-

rication with focused CO_2 laser pulses," Electron. Lett. **34,** 302–303 (1998).
4. G. Rego, O. Okhotnikov, E. Dianov, and V. Sulimov, "High-temperature stability of long-period fiber gratings produced using an electric arc," J. Lightwave Technol. **19,** 1574–1579 (2001).
5. S. Savin, M. J. K. Digonnet, G. S. Kino, and H. J. Shaw, "Tunable mechanically induced long-period fiber gratings," Opt. Lett. **25,** 710–712 (2000).
6. Y. Liu, J. A. R. Williams, L. Zhang, and I. Bennion, "Phase shifted and cascaded long-period fiber gratings," Opt. Commun. **164,** 27–31 (1999).
7. B. J. Eggleton, P. A. Krug, L. Poladian, and F. Ouellette, "Long periodic superstructure Bragg gratings in optical fibres," Electron. Lett. **30,** 1620–1622 (1994).
8. B. H. Lee, Y. Liu, S. B. Lee, S. S. Choi, and J. N. Jang, "Displacements of the resonant peaks of a long-period fiber grating induced by a change of ambient refractive index," Opt. Lett. **22,** 1769–1771 (1997).
9. H. J. Patrick, A. D. Kersey, and F. Bucholtz, "Analysis of the response of long period fiber gratings to external index of refraction," J. Lightwave Technol. **16,** 1606–1612 (1998).
10. X. Shu, X. Zhu, S. Jiang, W. Shi, and D. Huang, "High sensitivity of dual resonant peaks of long-period fibre gratings to surrounding refractive index changes," Electron. Lett. **35,** 1580–1581 (1999).
11. B. A. L. Gwandu, X. Shu, T. D. P. Allsop, W. Zhang, L. Zhang, and I. Bennion, "Simultaneous refractive index and temperature measurement using cascaded long-period grating in double-cladding fibre," Electron. Lett. **38,** 695–696 (2002).
12. O. Duhem, J. F. Henninot, and M. Douay, "Study of in fiber Mach–Zehnder interferometer based on two spaced 3-dB long period gratings surrounded by refractive index higher than that of silica," Opt. Commun. **180,** 255–262 (2000).
13. P. L. Swart, "Long-period grating Michelson refractometric sensor," Meas. Sci. Technol. **15,** 1576–1580 (2004).
14. H. Ke, K. S. Chiang, and J. H. Peng, "Analysis of phase-shifted long-period fiber gratings," IEEE Photonics Technol. Lett. **10,** 1596–1598 (1988).
15. G. Humbert and A. Malki, "High performance bandpass filters based on electric arc-induced π-shifted long-period fibre gratings," Electron. Lett. **39,** 1506–1507 (2003).
16. D. A. Pereira, O. Frazão, and J. L. Santos, "Fibre Bragg grating sensing system for simultaneous measurement of salinity and temperature," Opt. Eng. **43,** 299–304 (2004).
17. O. Esteban, M. Cruz-Navarrete, A. González-Cano, and E. Bernabeu, "Measurement of the degree of salinity of water with a fiber-optic sensor," Appl. Opt. **38,** 5267–5271 (1999).
18. X. Quan and E. S. Fry, "Empirical equation for the index of refraction of seawater," Appl. Opt. **34,** 3477–3480 (1995).
19. G. Rego, R. Falate, H. J. Kalinowski, J. L. Fabris, P. V. S. Marques, H. M. Salgado, and J. L. Santos, "Simultaneous temperature and strain measurements based on arc-induced long-period fiber gratings," in *17th International Conference on Optical Fiber Sensors,* M. Voet, R. Willsch, W. Ecke, J. Jones, and B. Culshaw, eds., Proc. SPIE **5855,** 679–682 (2005).